$^{13}C-^{1}H$ Spin-Coupling Constants in the β-D-Ribofuranosyl Ring: Effect of Ring Conformation on Coupling Magnitudes

Carol A. Podlasek,[†] Wayne A. Stripe,[†] Ian Carmichael,[‡] Maoyu Shang,[†] Bidisa Basu,[†] and Anthony S. Serianni*,[†]

Contribution from the Department of Chemistry and Biochemistry and the Radiation Laboratory, University of Notre Dame, Notre Dame, Indiana 46556

Received June 16, 1995[⊗]

Abstract: Experimental and computational methods have been used to examine the behavior of one-, two-, and three-bond $^{13}C-^{1}H$ spin-coupling constants ($^{1}J_{CH}$, $^{2}J_{CH}$ and $^{3}J_{CH}$, respectively) within the β-D-ribofuranosyl ring **1** that may be potentially affected by ring conformation. *Ab initio* molecular orbital (MO) calculations at the HF/6-31G* and MP2/6-31G* levels of theory were employed to assess the effect of ring conformation on molecular parameters (i.e., bond lengths, angles, and torsions) of β-D-ribofuranose (**2**) and methyl β-D-ribofuranoside (**3**), and these data were validated through comparison to corresponding parameters obtained by X-ray crystallography. The MO-derived structural data were subsequently used to compute $^{1}J_{CH}$, $^{2}J_{CH}$ and $^{3}J_{CH}$ values in **2** as a function of ring conformation. This predicted behavior was then tested experimentally through the measurement of J_{CH} values in conformationally-rigid model compounds (aldopyranosides) containing $^{13}C-^{1}H$ coupling pathways similar to those found in specific conformers of **2** and was examined for consistency with previously-derived empirical rules correlating J_{CH} with structure in carbohydrates. Available J_{CH} data obtained on several biologically-important compounds containing β-D-ribofuranosyl rings have been interpreted in light of the new correlations with ring conformation.

Introduction

Aldofuranosyl rings having the β-D-*ribo* configuration **1** are common constituents of biologically-important molecules, most notably RNA. Structure **1**, either as a singular entity or component of more complex molecules, can exist in various conformations in solution,[1−5] and thus significant conformational flexibility (internal motion) can be conferred to molecules containing **1** as a constituent. This flexibility may have important consequences for recognition processes *in vivo*,[6] and thus its character has been of interest to structural biologists.

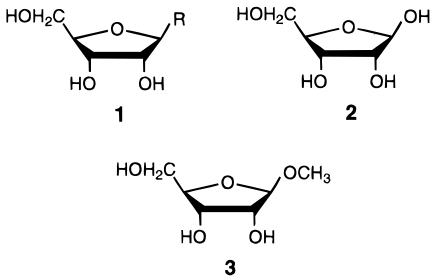

Scheme 1. Pseudorotational Itinerary of an Aldofuranose Ring

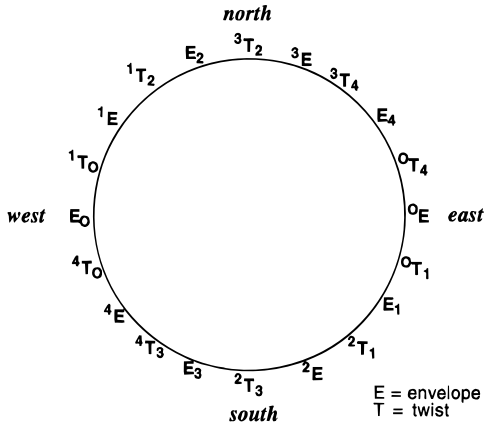

In structures like RNA, a two-state model[7] is usually invoked to describe the conformational behavior of its constituent β-D-ribofuranosyl rings. This model assumes a dynamic interconversion between north (N) and south (S) nonplanar forms of **1**, with ^{3}E and ^{2}E taken as the representative N and S forms, respectively. $^{3}E \leftrightarrow {}^{2}E$ interconversion may occur via two pathways, inversion[1a] or pseudorotation.[7] In the former, interconversion involves the planar (P) form; thus, $^{3}E \leftrightarrow P \leftrightarrow {}^{2}E$. In pseudorotation,[7] the interconversion occurs via nonplanar forms (Scheme 1). Since the P form is considered less stable (more strained) than nonplanar forms of **1**, pseudorotation appears to be the more favored mechanism. Of the two routes available for N/S interconversion via pseudorotation, the east pathway ($^{3}E \leftrightarrow E_4 \leftrightarrow {}^{0}E \leftrightarrow E_1 \leftrightarrow {}^{2}E$) appears more preferred than the west ($^{3}E \leftrightarrow E_2 \leftrightarrow {}^{1}E \leftrightarrow E_0 \leftrightarrow {}^{4}E \leftrightarrow E_3 \leftrightarrow {}^{2}E$)[1b,3,5a] since fewer nonbonded interactions (notably between substituents at C1 and C4) are present in east forms.

* To whom correspondence should be addressed.
† Department of Chemistry and Biochemistry.
‡ Radiation Laboratory.
⊗ Abstract published in *Advance ACS Abstracts,* December 1, 1995.

(1) (a) Westhof, E.; Sundaralingam, M. *J. Am. Chem. Soc.* **1983**, *105*, 970−976. (b) Levitt, M.; Warshel, A. *J. Am. Chem. Soc.* **1978**, *100*, 2607−2613.

(2) Westhof, E.; Sundaralingam, M. *J. Am. Chem. Soc.* **1980**, *102*, 1493−1500.

(3) Olson, W. K. *J. Am. Chem. Soc.* **1982**, *104*, 278−286.

(4) Olson, W. K.; Sussman, J. L. *J. Am. Chem. Soc.* **1982**, *104*, 270−278.

(5) (a) Harvey, S. C.; Prabhakaran, M. *J. Am. Chem. Soc.* **1986**, *108*, 6128−6136. (b) Pearlman, D. A.; Kim, S.-H. *J. Biomol. Struct. Dyn.* **1985**, *3*, 99−124.

(6) Changes in the conformational flexibility of the furanose rings of RNA upon binding to appropriate receptors may affect the free energy of binding via changes in the free entropy of binding.

(7) Altona, C.; Sundaralingam, M. *J. Am. Chem. Soc.* **1972**, *94*, 8205−8212.

0002-7863/96/1518-1413$12.00/0

Table 1. One-, Two-, and Three-Bond $^{13}C-^{1}H$ Coupling Pathways in the β-D-Ribofuranosyl Ring **1**

intraring	hydroxymethyl
C1−H1	C3−H5*R*
C1−H2	C3−H5*S*
C1−H3	C4−H5*R*
C1−H4	C4−H5*S*
C2−H1	C5−H4
C2−H2	C5−H5*R*
C2−H3	C5−H5*S*
C2−H4	
C3−H1	
C3−H2	
C3−H3	
C3−H4	
C4−H1	
C4−H2	
C4−H3	
C4−H4	
C5−H3	

A number of theoretical and experimental studies appear to validate a two-state N/S conformational model for **1**. X-ray crystallographic studies conducted on ribonucleosides(tides)[8] reveal ring conformations lying in broad N and S domains, thus supporting the two-state model in the solid state. Studies in solution have relied heavily on three-bond $^{1}H-^{1}H$ spin-coupling constants ($^{3}J_{HH}$) as conformational probes.[9] Within **1**, three $^{3}J_{HH}$ values are available ($^{3}J_{H1,H2}$, $^{3}J_{H2,H3}$ and $^{3}J_{H3,H4}$), but $^{3}J_{H2,H3}$ has been shown[9] to be of limited value for conformational analysis. Thus, only $^{3}J_{H1,H2}$ and $^{3}J_{H3,H4}$ are available to test the validity of the two-state N/S model in solution. Clearly, this limited number of couplings is insufficient to discriminate between the many conformational models available to **1**. The fact that $^{3}J_{HH}$ values in **1** have been treated quantitatively using this model to compute the proportions of N and S populations[10] does not constitute definitive proof that the two-state N/S model is the only model consistent with the available couplings. Furthermore, most of the available $^{1}H-^{1}H$ internuclear distances in **1**, which are potentially accessible via NOE and/or relaxation measurements, are not sensitive enough for use in conformational analysis.[11] In addition, while the solution behavior of aldofuranosyl rings having the *β-ribo* configuration may be accurately described by a two-state N/S model, rings having other configurations (α-*ribo*; α,*β-arabino*; α,*β-lyxo*; α,*β-xylo*) may not behave in the same manner.

We have been interested in examining $^{13}C-^{1}H$ (and $^{13}C-^{13}C$) spin-couplings as alternative conformational probes of furanosyl rings in solution.[12−16] Within **1**, there are six $^{1}J_{CH}$, nine $^{2}J_{CH}$, and nine $^{3}J_{CH}$ values (Table 1), giving a total of twenty-four J_{CH} values that contain potentially useful structural information.[17] The magnitudes and signs of $^{13}C-^{1}H$ spin-couplings can be measured accurately in ^{13}C-labeled molecules using paired cross-peak displacements in 2D TOCSY[18,19] and 3D HMQC-TOCSY[20,21] spectra, and recent developments in the ^{13}C labeling of ribonucleosides[12] and RNA[22] promise to provide ready access to J_{CH} values within these structures. However, the relationships between J_{CH} values and ring conformation in **1** are not well defined at present,[12] thus compromising their use in structural studies.

This paper examines the behavior of $^{1}J_{CH}$, $^{2}J_{CH}$, and $^{3}J_{CH}$ values in **1** using theoretical and experimental approaches. We have conducted *ab initio* molecular orbital calculations on **2** to obtain a detailed picture of its structure (i.e., bond lengths, angles, torsions) as a function of conformation, and these data have been used to compute J_{CH} values as a function of ring geometry. These computational results were subsequently tested experimentally by measuring J_{CH} values in model compounds containing $^{13}C-^{1}H$ coupling pathways that mimic those found in discrete nonplanar conformations of **1** and **2**. These data provide a basis on which to evaluate the utility of particular J_{CH} values in **1** and **2** as conformational probes.

Experimental Section

Synthesis of ^{13}C-Labeled Aldopyranosides. ^{13}C-Labeled aldoses were prepared by methods described previously,[23−32] and thus only a brief description of their synthesis is provided here.

D-[1-^{13}C]Mannose, D-[1-^{13}C]allose, and D-[1-^{13}C]arabinose were prepared by cyanohydrin reduction,[23,24,28] using K^{13}CN and D-arabinose, D-ribose, and D-erythrose, respectively, as the starting aldoses.

D-[2-^{13}C]Mannose and D-[2-^{13}C]allose were prepared by molybdate-catalyzed epimerization[27] of D-[1-^{13}C]glucose and D-[1-^{13}C]altrose, respectively. The latter [1-^{13}C]hexoses were obtained as byproducts from the synthesis of D-[1-^{13}C]mannose and D-[1-^{13}C]allose, respectively.

D-[3-^{13}C]Mannose and D-[3-^{13}C]allose were prepared by cyanohydrin reduction,[23,24] using KCN and D-[2-^{13}C]arabinose and D-[2-^{13}C]ribose, respectively, as the starting aldoses. D-[2-^{13}C]Arabinose and D-[2-^{13}C]-ribose were obtained by molybdate-catalyzed epimerization of D-[1-^{13}C]ribose and D-[1-^{13}C]arabinose, respectively.[26] The latter [1-^{13}C]-pentoses were prepared by cyanohydrin reduction[23,25,26] using K^{13}CN and D-erythrose.

D-[4-^{13}C]Glucose was prepared chemi-enzymically from dihydroxyacetone phosphate (DHAP) and DL-[1-^{13}C]glyceraldehyde via aldolase-catalyzed aldol condensation.[29] DL-[1-^{13}C]Glyceraldehyde was prepared via cyanohydrin reduction using K^{13}CN and glycolaldehyde.[24] D-[5-^{13}C]Glucose was prepared as described for D-[4-^{13}C]glucose, but substituting DL-[2-^{13}C]glyceraldehyde in the aldolase reaction.[24] DL-[2-^{13}C]Glyceraldehyde was prepared by cyanohydrin reduction using

(8) (a) de Leeuw, H. P. M.; Haasnoot, C. A. G.; Altona, C. *Isr. J. Chem.* **1980**, *20*, 108−126.
(9) Altona, C.; Sundaralingam, M. *J. Am. Chem. Soc.* **1973**, *95*, 2333−2344.
(10) (a) Davies, D. B.; Danyluk, S. S. *Biochemistry* **1974**, *13*, 4417−4434. (b) Haasnoot, C. A. G.; de Leeuw, F. A. A. M.; de Leeuw, H. P. M.; Altona, C. *Org. Magn. Reson.* **1981**, *15*, 43−52.
(11) (a) Wüthrich, K. *NMR of Proteins and Nucleic Acids*; Wiley-Interscience: New York, 1986; p 208. (b) van de Ven, F. J. M.; Hilbers, C. W. *Eur. J. Biochem.* **1988**, *178*, 1−38.
(12) Kline, P. C.; Serianni, A. S. *J. Am. Chem. Soc.* **1990**, *112*, 7373−7381.
(13) Kline, P. C.; Serianni, A. S. *J. Org. Chem.* **1992**, *57*, 1772−1777.
(14) Bandyopadhyay, T.; Wu, J.; Serianni, A. S. *J. Org. Chem.* **1993**, *58*, 5513−5517.
(15) Vuorinen, T.; Serianni, A. S. *Carbohydr. Res.* **1990**, *209*, 13−31.
(16) Serianni, A. S.; Barker, R. *J. Org. Chem.* **1984**, *49*, 3292−3300.
(17) Serianni, A. S. In *NMR of Biological Macromolecules*; Stassinopoulou, C. I., Ed.; Springer-Verlag: 1994; NATO ASI Series H: Cell Biology, Vol. 87; pp 293−306.
(18) Montelione, G. T.; Winkler, M. E.; Rauenbuehler, P.; Wagner, G. *J. Magn. Reson.* **1989**, *82*, 198−204.
(19) Serianni, A. S.; Podlasek, C. A. *Carbohydr. Res.* **1994**, *259*, 277−282.
(20) Hines, J. V.; Varani, G.; Landry, S. M.; Tinoco, I., Jr. *J. Am. Chem. Soc.* **1993**, *115*, 11002−11003.
(21) Hines, J. V.; Landry, S. M.; Varani, G.; Tinoco, I., Jr. *J. Am. Chem. Soc.* **1994**, *116*, 5823−5831.
(22) Nikonowicz, E. P.; Sirr, A.; Legault, P.; Jucker, F. M.; Baer, L. M.; Pardi, A. *Nucl. Acids Res.* **1992**, *20*, 4507−4513.
(23) Serianni, A. S.; Nunez, H. A.; Barker, R. *Carbohydr. Res.* **1979**, *72*, 71−78.
(24) Serianni, A. S.; Clark, E. L.; Barker, R. *Carbohydr. Res.* **1979**, *72*, 79−91.
(25) Serianni, A. S.; Vuorinen, T.; Bondo, P. B. *J. Carbohydr. Chem.* **1990**, *9*, 513−541.
(26) Serianni, A. S.; Bondo, P. B. *J. Biomol. Struct. Dyn.* **1994**, *11*, 1133−1148.
(27) Hayes, M. L.; Pennings, N. J.; Serianni, A. S.; Barker, R. *J. Am. Chem. Soc.* **1982**, *104*, 6764−6769.
(28) King-Morris, M. J.; Serianni, A. S. *J. Am. Chem. Soc.* **1987**, *109*, 3501−3508.
(29) Serianni, A. S.; Cadman, E.; Pierce, J.; Hayes, M. L.; Barker, R. *Methods Enzymol.* **1982**, *89* (Part D), 83−92.

Table 2. Crystal Data and Experimental Details for Methyl β-D-Ribofuranoside **3**

formula	$C_6H_{12}O_5$
FW	164.16
F(000)	704
ω width at half-height, deg	0.20
Mo Kα radiation, Å	$\lambda = 0.710\ 73$
crystal dimensions, mm	$0.33 \times 0.16 \times 0.11$
temperature, °C	20
space group	$P2_12_12_1$
a, Å	4.8595(7)
b, Å	24.162(5)
c, Å	12.876(2)
V, Å	1511.8(5)
Z	8
calcd density, g/cm^{-3}	1.442
μ (Mo Kα), cm^{-1}	1.185
instrument	Enraf-Nonius CAD4 diffractometer
monochromator	graphite crystal, incident beam
attenuator	Zr foil, factor 19.291
take-off angle, deg	2.8
detector aperture	1.8−2.4 mm horizontal 4.0 mm vertical
crystal-detector dist, cm	21
scan type	$\omega/2\theta$
scan rate, deg/min	5.49−1.27 (in ω)
scan width, deg	$0.6 + 0.340 \tan(\theta)$
maximum 2θ, deg	60.0
no. of refl measured	4428 total, 4368 unique
corrections	Lorentz-polarization ψ curve absorption (trans: 0.9774−0.9978)
solution	direct methods
hydrogen atoms	located and refined isotropically
refinement	full-matrix least-squares
minimization function	$\sum w(\lvert F_o\rvert - \lvert F_c\rvert)^2$
least-squares weights	$4F_o^2\sigma^2(F_o^2) = 1/\sigma^2(F_o)$
anomalous dispersion	all non-hydrogen atoms
reflections included	3511 with $F_o^2 > 3.0\sigma(F_o^2)$
parameters defined	295
unweighted agreement factor	0.03459
weighted agreement factor	0.04304
ESD of obsd unit weight	1.283
convergence, largest shift	0.001
high peak in final diff map, e/Å^3	0.261(5)
low peak in final diff map, e/Å^3	−0.284(5)
computer hardware	VAXstation 3200
computer software	SDP/VAX

KCN and [1-^{13}C]glycolaldehyde;[24] the latter was prepared from K^{13}CN and formaldehyde.[24]

D-[5-^{13}C]Arabinose was prepared from D-[6-^{13}C]glucose by treatment of the latter with $Pb(OAc)_4$ to give D-[4-^{13}C]erythrose,[16] followed by chain extension of the labeled tetrose via cyanohydrin reduction to give the [5-^{13}C]pentoses.[26,30] D-[6-^{13}C]Glucose was prepared from 1,2-*O*-isopropylidene-α-D-*xylo*-pentodialdo-1,4-furanose and K^{13}CN as described previously.[31]

After purification, the ^{13}C-labeled aldoses were converted to their corresponding methyl glycosides via Fischer glycosidation using Dowex 50 × 8 (20−50 mesh) (H^+ form) ion-exchange resin as the catalyst,[32] and the appropriate aldopyranoside anomer was isolated via column chromatography on Dowex 1 × 2 (200−400 mesh) ion-exchange resin in the hydroxide form.[32,33]

X-ray Crystallography. Colorless column-shaped crystals of methyl β-D-ribofuranoside **3** were obtained by vapor diffusion of toluene into a solution of **3** in ethyl acetate over a 4-week period at 4 °C. A single crystal was mounted on a glass fiber with the long axis approximately parallel to the goniometer head axis. Preliminary examination and data collection were performed with Mo Kα radiation on an Enraf-Nonius CAD4 computer-controlled kappa axis diffractometer equipped with a graphite crystal, incident beam monochromator. Crystal data and experimental details of the structure determination are given in Table 2. The structure was solved by direct methods[34] which revealed coordinates for two sets of five-membered rings (molecules A and B). Positional and equivalent isotropic thermal parameters for these crystal forms of **3** are provided as supporting information.

Scheme 2. Initial C−O Rotamers Used in *ab Initio* MO Calculations on **2**

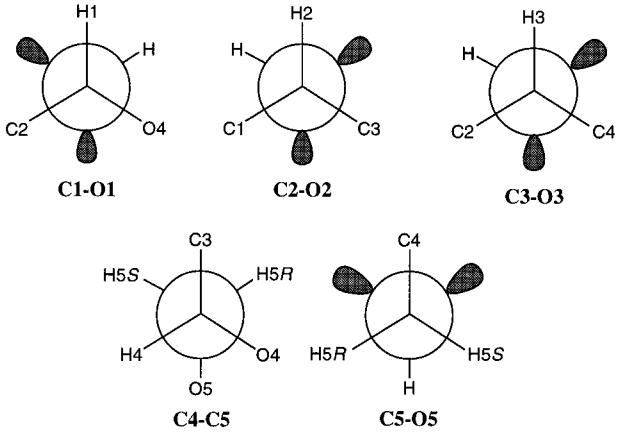

NMR Spectroscopy. ^{1}H NMR spectra were obtained on Varian VXR-500S (UNITY) and Varian UNITY-Plus 600 MHz FT-NMR spectrometers operating at 499.843 and 599.888 MHz, respectively, for ^{1}H. Spectra were collected on ∼30 mM aqueous (^2H_2O) solutions at 30 °C. One-dimensional ^{1}H NMR spectra were obtained with a digital resolution of 0.02 Hz/point and were processed with resolution enhancement in order to facilitate the measurement of small J_{CH} values.

2D TOCSY spectra were obtained with a 2K × 2K data matrix, which was processed to a final matrix size of 4K × 4K. A sine-bell function was applied to the F_1 dimension prior to fourier transformation. $^{13}C-^{1}H$ spin-couplings in ^{13}C-labeled molecules were measured by the ^1J-resolved cross-peak displacement method;[18,19] digital resolution in TOCSY data allowed the measurement of J_{CH} values to within ± 0.2 Hz.

***Ab Initio* Molecular Orbital Calculations.** *Ab initio* molecular orbital (MO) calculations were conducted (Gaussian 92)[35] on β-D-ribofuranose **2** using the Hartree−Fock (HF) procedure and a polarized split-valence basis set (6-31G*). Ten envelope conformers (^{3}E, E$_4$, ^{0}E, E$_1$, ^{2}E, E$_3$, ^{4}E, E$_0$, ^{1}E, and E$_2$) and the planar (P) conformer were examined as described previously[36−38] by constraining the appropriate endocyclic torsion angle within **2** to 0° (thus, for example, in ^{3}E, the C4−O4−C1−C2 dihedral angle was fixed at 0°); two endocyclic torsions were fixed at 0° in calculations on the P form. All other geometric parameters (i.e., bond lengths, angles, and torsions) were optimized in the calculations.

The choice of initial exocyclic C−C and C−O torsions (C1−O1, C2−O2, C3−O3, C4−C5, C5−O5) (Scheme 2) was arbitrary except

(30) Wu, J.; Bondo, P. B.; Vuorinen, T.; Serianni, A. S. *J. Am. Chem. Soc.* **1992**, *114*, 3499−3505.

(31) King-Morris, M. J.; Bondo, P. B.; Mrowca, R. A.; Serianni, A. S. *Carbohydr. Res.* **1988**, *175*, 49−58.

(32) Podlasek, C. A.; Wu, J.; Stripe, W. A.; Bondo, P. B.; Serianni, A. S. *J. Am. Chem. Soc.* **1995**, *117*, 8635−8644.

(33) Austin, P. W.; Hardy, F. E.; Buchanan, J. C.; Baddiley, J. *J. Chem. Soc.* **1963**, 5350−5353.

(34) Main, P.; Fiske, S. J.; Hull, S. E.; Lessinger, L.; Germain, G.; DeClercq, J.-J.; Woofson, M. M. *MULTAN 11/82*, University of York: York, England, 1982.

(35) Frisch, M. J.; Trucks, G. W.; Head-Gordon, M.; Gill, P. M. W.; Wong, M. W.; Foresman, J. B.; Johnson, B. G.; Schlegel, H. B.; Robb, M. A.; Replogle, E. S.; Gomperts, R.; Andres, J. L.; Raghavachari, K.; Binkley, J. S.; Gonzales, C.; Martin, R. L.; Fox, D. J.; DeFrees, D. J.; Baker, J.; Stewart, J. J. P.; Pople, J. A. *Gaussian 92, Revision C.3*; Gaussian, Inc.: Pittsburgh, PA, 1992.

(36) Serianni, A. S.; Chipman, D. M. *J. Am. Chem. Soc.* **1987**, *109*, 5297−5303.

(37) Garrett, E. C.; Serianni, A. S. *Carbohydr. Res.* **1990**, *206*, 183−191.

(38) Garrett, E. C.; Serianni, A. S. In *Computer Modeling of Carbohydrate Molecules*; ACS Symposium Series No. 430; French, A. D., Brady, J. W., Eds.; American Chemical Society: Washington, DC, 1990; pp 91−119.

for the C1−O1 torsion, which was chosen to optimize the exoanomeric effect,[39a,b] as described in previous reports;[36−38] the full energy surface for **2** was not examined since $3^5 \times 11 = 2673$ unique structures would need to be studied, which was not deemed practical given present computer limitations. However, some insights into the effects of these torsions on structure were obtained and are reported herein. It should be appreciated that these calculations pertain to unsolvated, "gas-phase" structures (i.e., solvent effects have not been treated), since at present it is not possible to include solvation effects, either implicitly by a suitably configured dielectric reaction field or explicitly by selecting and locating a suitable number of solvent molecules, in *ab initio* calculations with reasonable confidence.

Computations on methyl β-D-ribofuranoside **3** were confined to a single ring geometry, corresponding to that observed for molecule B in the crystal, by fixing the endocyclic torsion angle, C3−C4−O4−C1, at −3.38°. All exocyclic torsion angles (C1−O1, C2−O2, C3−O3, C4−C5, C5−O5) were set at initial values similar to those observed in molecule B, but these torsions were allowed to optimize during the calculation. All other molecular parameters were optimized with the exception of the O1−CH_3 torsion, which was fixed in an ideal staggered conformation. For **3**, computations were conducted at the HF/6-31G* and MP2/6-31G* levels of theory.

Calculations of ^{13}C−^{1}H Spin-Coupling Constants. ^{13}C−^{1}H spin-coupling constants were obtained by finite (Fermi-contact) field double perturbation theory calculations[40a] at the HF and MP2 levels using a basis set designed for the economical recovery of such properties.[40b] Scale factors have been developed for this basis set for $^1J_{CC}$, $^1J_{CH}$, $^2J_{CH}$, and $^3J_{CH}$ which allow the reliable prediction of results expected at a much higher level of theory, namely quadratic configuration interaction (QCISD).[40c] The scale factors were estimated from the equation $f_n = [^nJ_{CH}(\text{QCISD}) - {}^nJ_{CH}(\text{HF})]/[^nJ_{CH}(\text{MP2}) - {}^nJ_{CH}(\text{HF})]$, in systems where the full QCISD calculation is possible. Values of $f_1 = 0.83$, $f_2 = 0.75$, and $f_3 = 0.83$ were obtained for the present basis set which may be written [5s2p1d|2s]. These values allow the estimation of $^nJ_{CH}$(QCISD) values in much larger systems for which only the HF and MP2 calculations are at present tractable. It should be observed that *trends* in the computed coupling constants are already reproduced at the HF level, whereas the absolute magnitudes are poorly estimated due to the neglect of electron correlation. The importance of these electron correlation effects is overestimated in the simplest recovery scheme (MP2), so that comparison with more complete treatments (QCISD) leads to scale factors less than unity.

Results and Discussion

1. *Ab Initio* Calculations on β-D-Ribofuranose 2. The *ab initio* MO data were used to provide information on the conformational energies of the various nonplanar forms of **2** and on the behavior of individual molecular parameters in these forms. These features are discussed separately below.

A. Conformational Energies. The effect of ring conformation of **2** on total energy is shown in Figure 1. Smooth energy transitions are observed between the 10 envelope (E) forms, with the global energy minimum located at E_2 (N form) and a local minimum at ^{2}E (S form). In E_2, the C1−O1 and C2−O2 bonds are quasi-axial, whereas C3−O3 and C4−C5 are quasi-equatorial, an arrangement that is apparently more stable (in the gas-phase) than that having C1−O1, C2−O2, and C4−C5 quasi-equatorial and C3−O3 quasi-axial (^{2}E), at least for the particular combination of exocyclic torsions tested. The computed energy difference between ^{2}E and E_2 is 2.4 kcal/mol. In contrast, the planar (P) form of **2** is 6.5 kcal/mol less stable than E_2. The energy barrier to N/S exchange is ∼3.7 kcal/mol via the east pathway (the west barrier is ∼4.4 kcal/mol); both barriers are lower than N/S exchange via the P form, providing evidence that pseudorotation is more preferred than inversion. These results differ somewhat from those obtained previously on β-D-ribofuranosyl rings using semiempirical methods.[3,5a] The energy difference between ^{2}E and E_2 in the present calculation is larger than those obtained by Olson[3] and Harvey and Prabhakaran;[5a] the latter studies report values < 0.5 kcal/mol. N/S barrier heights via east and west pathways have been reported previously[3] to be ∼3.8 and ∼7.8 kcal/mol, respectively; the former value is similar to that obtained in this study. It should be noted, however, that Olson[3] employed a 5-deoxy-β-D-ribofuranosylamine in calculations of conformational energies where the presence of a CH_3 group at C4 (instead of CH_2OH) and the amino group at C1 could affect N/S energetics. Furthermore, exocyclic bond torsions, most notably C4−C5, will probably affect the relative energies of conformers, but only one of 3^5 possible combinations of these torsions was examined in this work. Finally, the neglect of electron correlation effects appears to give slightly larger energy barriers for pseudorotation.[41]

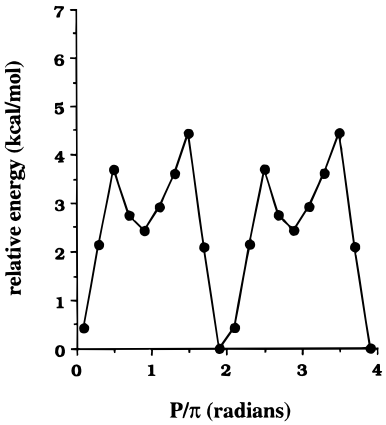

Figure 1. Relative energies of the 10 envelope (E) and planar forms of **2** derived from *ab initio* molecular orbital calculations (HF/6-31G*). One cycle of the pseudorotational itinerary is defined as 0−2 P/π radians, with 0.1 $P/\pi = {}^3$E (Scheme 1).

B. Bond Lengths. The C−H bond lengths (ring carbons) in **2** are sensitive to ring conformation (Figure 2). The behavior of the C1−H1, C2−H2, and C4−H4 bonds is consistent with observations reported in other aldofuranosyl rings,[36−38,41] that is, a particular C−H bond is longer when quasi-axial than when quasi-equatorial. Interestingly, the C3−H3 bond shows the opposite effect (Figure 2B), but this aberation has been attributed to O3 lone-pair effects caused by significant C3−O3 bond rotation during geometric optimization[41] (see below).

Exocyclic C−O bonds (C1−O1, C2−O2, and C3−O3) also change systematically in length with ring conformation, with a particular C−O bond shorter when quasi-equatorial than when quasi-axial (e.g., C2−O2 is shorter in ^{2}E than in E_2) (Figure 3A). The exocyclic C4−C5 bond exhibits similar behavior, being shorter in E_4 (quasi-equatorial) than in ^{4}E (quasi-axial) (Figure 3B). Thus, the correlation between orientation (quasi-axial/quasi-equatorial) and exocyclic bond length is observed not only for C−H bonds, as reported recently,[41] but also for C−O and C−C bonds in the β-D-ribofuranosyl ring and possibly in aldofuranosyl rings having other configurations.

The two endocyclic C−O bonds, C1−O4 and C4−O4, also change in length with ring conformation (Figure 3C). The C1−O4 bond is shortest in E_0−^{1}E forms where the C1−O1 bond is

(39) (a) Lemieux, R. U. *Pure Appl. Chem.* **1971**, *25*, 527−548. (b) Lemieux, R. U.; Koto, S.; Voisin, D. In *Anomeric Effect: Origin and Consequences*; ACS Symposium Series, No. 87; Szarek, W. A., Horton, D., Eds.; American Chemical Society: Washington, DC, 1979; pp 17−29.

(40) (a) Kowalewski, J.; Laaksonen, A.; Roos, B.; Siegbahn, P. *J. Chem. Phys.* **1979,** *71*, 2896−2902. (b) Carmichael, I. *J. Phys. Chem.* **1993**, *97*, 1789−1792. (c) Pople, J. A.; Head-Gordon, M.; Raghavachari, K. *J. Chem. Phys.* **1987**, *87*, 5968−5975.

(41) Serianni, A. S.; Wu, J.; Carmichael, I. *J. Am. Chem. Soc.* **1995**, *117*, 8645−8650.

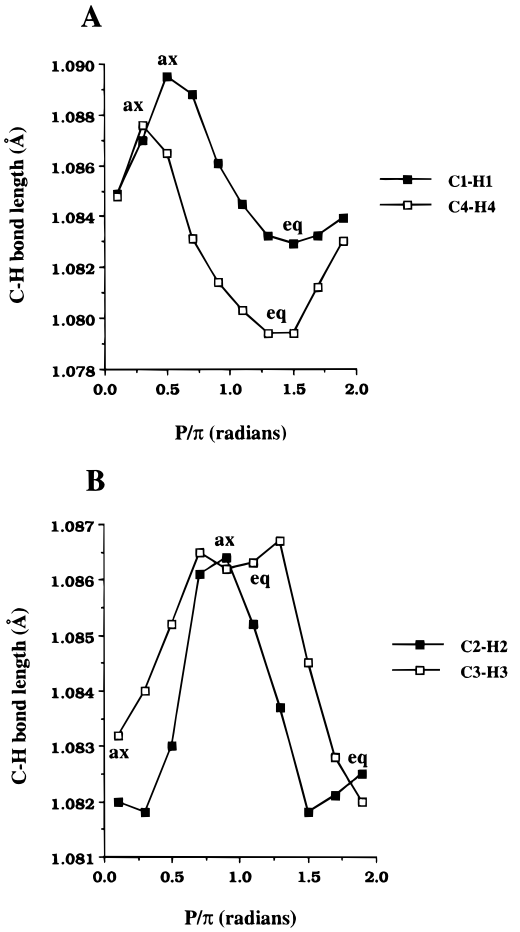

Figure 2. The effect of ring conformation of **2** on C1−H1 and C4−H4 bond lengths (A) and C2−H2 and C3−H3 bond lengths (B).

quasi-axial; in this orientation, the anomeric effect[42] is optimal and lone-pair donation from O4 into the C1−O4 bond (lone pair → σ^*) is expected, resulting in a shortening of the C1−O4 bond and a lengthening of the C1−O1 bond as observed. The behavior of the C4−O4 bond is less readily explained, although minima are observed in conformations having O4 out of plane (Figure 3C).

C. C−O Bond Torsions. During geometric optimization of the ten E forms of **2**, the initial torsion angles chosen for the C1−O1 and C2−O2 bonds did not experience major changes (Figure 4A); the C1−O1 and C2−O2 torsions varied from 61° to 76° and from −45° to −61°, respectively. In contrast, the C3−O3 torsion changed significantly (Figure 4A). This latter behavior is attributed to the influence of intramolecular H-bonding between the *cis* hydroxyl groups at C2 and C3, which affects the optimal C2−O2 and C3−O3 torsion angles within each E form. This rotation changes the orientation of the lone pairs on O3 with respect to the C3−H3 bond in each E form and is responsible for the unusual behavior of the C3−H3 bond length in different forms (see above). As discussed earlier,[41] a lone pair *anti* to a given C−H bond (as found in S forms where the C3−H3 bond is quasi-equatorial) induces a lengthening of this bond, and this effect apparently supercedes the orientational effects discussed above.

D. Other Structural Parameters. Several other structural parameters vary with ring conformation of **2** and are worthy of comment. The C4−O4−C1 bond angle (∠C4−O4−C1) varies as shown in Figure 4B; this angle is minimal in ^{0}E, with a local

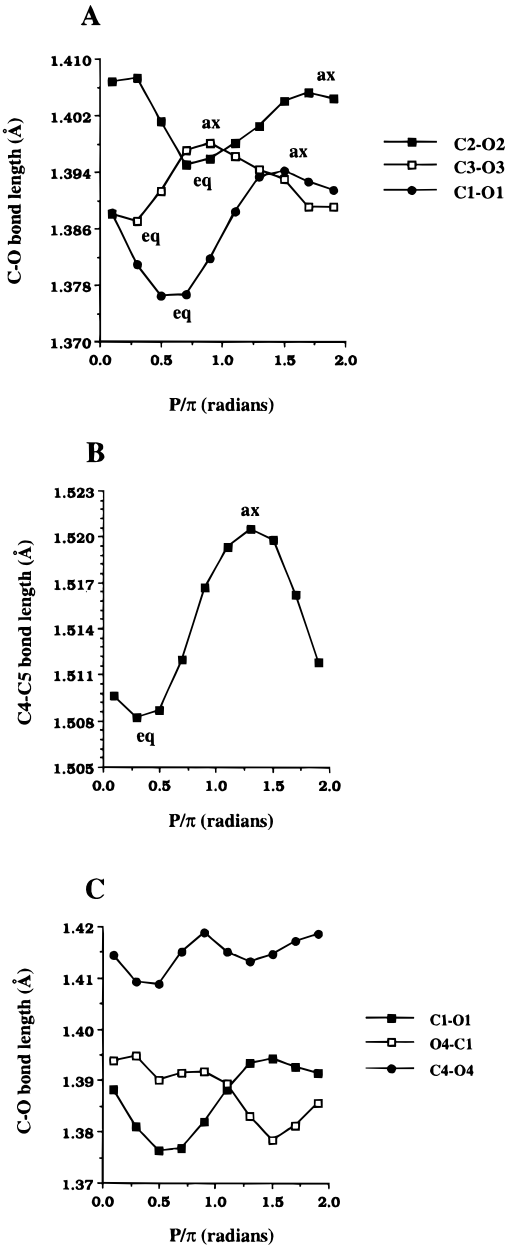

Figure 3. The effect of ring conformation of **2** on selected bond lengths: (A) C1−O1, C2−O2, and C3−O3; (B) C4−C5; (C) C1−O1, C1−O4, and C4−O4.

minimum near E_0. These minima are expected in conformations having O4 out of plane,[2,5a] but the difference in ∠C4−O4−C1 between E_0 and ^{0}E is not as well appreciated. Apparently, in ^{0}E in which the substituents at C1 and C4 are both quasi-equatorial, there is no need to maximize ∠C4−O4−C1 in order to reduce destabilizing 1,3-interactions, in contrast to E_0 where such destabilization is more pronounced.

The extent to which the out-of-plane atoms in E forms of **2** deviate from the ring plane is not constant throughout the pseudorotational itinerary. The angles that out-of-plane atoms make with the ring plane (e.g., for E_1, the C3−C4−O4−C1 torsion angle) range from 17 to 27° (Figure 5A). These angles have been converted to the pseudorotational parameter, τ_m (puckering amplitude) (Figure 5B), which agree well with those observed for β-D-ribofuranosyl rings of nucleosides in the crystalline state (∼38°),[2,7,8a] indicating that the HF/6-31G* level of theory provides a reasonable estimation of this parameter. It is interesting to note that ring puckering is, on average, greater in the eastern hemisphere than in the western hemisphere of

(42) Lemieux, R. U. In *Molecular Rearrangements*; de Mayo, P., Ed.; Wiley-Interscience: New York, 1963; p 713.

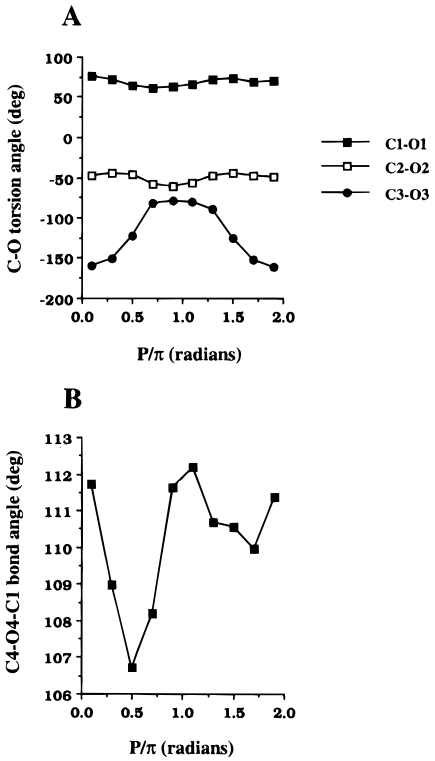

Figure 4. (A) The effect of ring conformation of **2** on the exocyclic C1−O1, C2−O2, and C3−O3 torsion angles. (B) The effect of ring conformation of **2** on the endocyclic C4−O4−C1 bond angle.

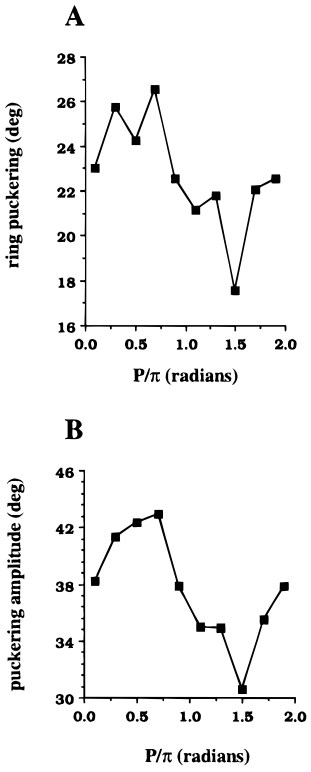

Figure 5. The effect of ring conformation of **2** on (A) ring puckering and (B) ring puckering amplitude τ_m.

the pseudorotational itinerary (Scheme 1) and that the puckering minimum occurs at E_0; these results are consistent with those obtained by Harvey and Prabhakaran.[5a] This latter minimum is expected since minimizing puckering at E_0 reduces the destabilizing effects of 1,3-interactions at C1 and C4 in this form.

E. Comparison to Crystal Structure. In order to evaluate potential errors in computed molecular parameters obtained at the HF/6-31G* level of theory, experimental molecular parameters (bond lengths, angles, and torsions) were obtained on methyl β-D-ribofuranoside **3** via X-ray crystallography. The unit cell contained two distinct forms of **3**, denoted molecules A and B (Figure 6). Both forms adopt a conformation near E_2 (north) ($P = -10.4°$ and $-24.3°$); interestingly, the HF/6-31G* computations on **2** revealed a global energy minimum at the same conformation (Figure 1). A comparison was made between molecular parameters in molecule B and computed parameters obtained on **3** at the HF/6-31G* and MP2/6-31G* levels of theory. In the computed structures, the C3−C4−O4−C1 torsion angle was held constant at $-3.38°$ to coincide with that observed in the crystal, and the CH_3 group was fixed in an ideal staggered rotamer; all other degrees of freedom in **3** were optimized.

Some representative molecular parameters are compared in Table 3. In general, the agreement between computed and crystal structures is fair, with better agreement observed at the MP2/6-31G* level, especially for C−O bond lengths. Particular attention was paid to structure in the vicinity of the anomeric carbon. In molecule B, $r_{C4-O4} > r_{C1-O1} > r_{C1-O4}$, whereas in the computed structures, $r_{C4-O4} > r_{C1-O4} \approx r_{C1-O1}$. However, the relative lengths of these bonds *in molecule A* is $r_{C4-O4} > r_{C1-O4} > r_{C1-O1}$, *in agreement with the computations*, suggesting that subtle changes in structure may notably affect these relative lengths. Interestingly, O4 and O1 in molecule A do not participate in H-bonding to other molecules in the crystal lattice, *unlike the corresponding atoms in molecule B.* We cannot assess whether the relative bond lengths observed in molecule A would be observed in molecule B if O1 and O4 in the latter were not participating in H-bonding (as in the computed structures). It is possible that H-bonding affects the electronic characteristics in the C4−O4−C1−O1 fragment and thus relative bond lengths. For this reason, it is unclear whether the generally better agreement between C−O bond lengths in molecule B and the computed MP2/6-31G* structure is actually meaningful, since O2, O3, and O5 in the former are also involved in the H-bonding network of the crystal.

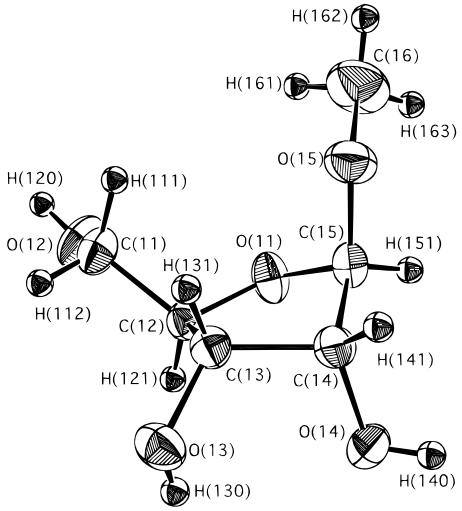

Figure 6. ORTEP diagram of the X-ray crystal structure of **3** (molecule B).

The C1−O1 torsions, ring puckerings and ∠C4−O4−C1 observed in X-ray and computed structures are in reasonable agreement (Table 3). Values of τ_m for molecules A and B in the crystal are 39.8° and 35.8°, respectively.

Thus, notwithstanding the many sources of error that may potentially compromise a comparison between the X-ray and

Table 3. Structural Parameters from Crystal Structure (Molecule B) and Molecular Orbital Calculations of Methyl β-D-Ribofuranoside **3** (E_2 Conformer)

parameter	crystal	HF/6-31G*	MP2/6-31G*
	Bond Lengths		
C1−C2	1.515		
C2−C3	1.526	1.5268	1.5269
C3−C4	1.531	1.5403	1.5409
C4−O4	1.439	1.4175	1.4455
C1−O4	1.405	1.3864	1.4123
C1−O1	1.419	1.3840	1.4105
C2−O2	1.412	1.4045	1.4278
C3−O3	1.412	1.3893	1.4130
C5−O5	1.421	1.4000	1.4239
C4−C5	1.502	1.5123	1.5082
	Bond Angles		
C4−O4−C1	109.7	111.20	108.75
	Bond Torsions		
H1−C1−O1−CH_3	58.04	55.88	58.50
H2−C2−O2−H	−29.94[b]	−50.84	−50.63
H3−C3−O3−H	179.58[b]	−160.75	−160.12
O5−C5−C4−C3	−176.00	−173.17	−174.69
C4−C5−O5−H	−174.63	−178.79	−179.88
C3−C4−O4−C1	−3.38	−3.38[a]	−3.38[a]
C2−C3−C4−O4	−19.15	−20.19	−21.46

[a] Torsion angle held constant in the MO calculations. [b] The observed difference between the crystal and computed values for these torsions is apparently due to hydrogen-bonding constraints imposed by the crystalline lattice.

computed structures of **3**, we conclude that the agreement is acceptable and that computed structures at the HF/6-31G* level are sufficiently reliable for use in the following analyses.

2. Internuclear $^{1}H-^{1}H$ Distances in 2. Six $^{1}H-^{1}H$ internuclear distances exist within the furanosyl ring of **2** that might serve as useful conformational probes:[11] H1−H2, H1−H3, H1−H4, H2−H3, H2−H4, and H3−H4. Using the MO-optimized envelope structures of **2** (see above), these distances were plotted as a function of ring conformation (Figure 7). Inspection of these data reveals that only r_{H1-H4} is sufficiently sensitive to ring conformation (Figure 7A). Moreover, the fact that only one $^{1}H-^{1}H$ distance is conformation-sensitive severely compromises its use in practical terms *when conformational averaging is present.* Due to the r^{-6} dependence of relaxation times and NOE, distances derived via these parameters in conformationally-mobile molecules will not be averaged linearly.[43,44] Thus, that (those) conformer(s) in which H1 and H4 lie close in space will be weighted disproportionately in the determination, thus compromising the use of this distance to assess complex conformational behavior in solution. We take this result as a rationale to further develop J_{CH} values as alternative structural probes.

3. H−H and C−H Torsion Angles in 2 and Their Relationship to $^{3}J_{HH}$ and $^{3}J_{CH}$ Values. It is well recognized[9] that the H1−C1−C2−H2, H2−C2−C3−H3, and H3−C3−C4−H4 torsion angles (Θ) in **2** are critical determinants of $^{3}J_{H1,H2}$, $^{3}J_{H2,H3}$, and $^{3}J_{H3,H4}$ values in **2**. The oscillation of $\Theta_{H2,H3}$ about ±40° makes $^{3}J_{H2,H3}$ a relatively insensitive conformational probe, whereas $\Theta_{H1,H2}$ and $\Theta_{H3,H4}$ vary from about 85° to 165°. Use of a parameterized Karplus relationship developed by Haasnoot *et al.*[45] permits the conversion of these torsions to $^{3}J_{HH}$ values as discussed previously.[12] The latter curves show that $^{3}J_{H1,H2}$ and $^{3}J_{H3,H4}$ are largest in S and N forms, respectively, and this complementarity has been exploited in estimations of

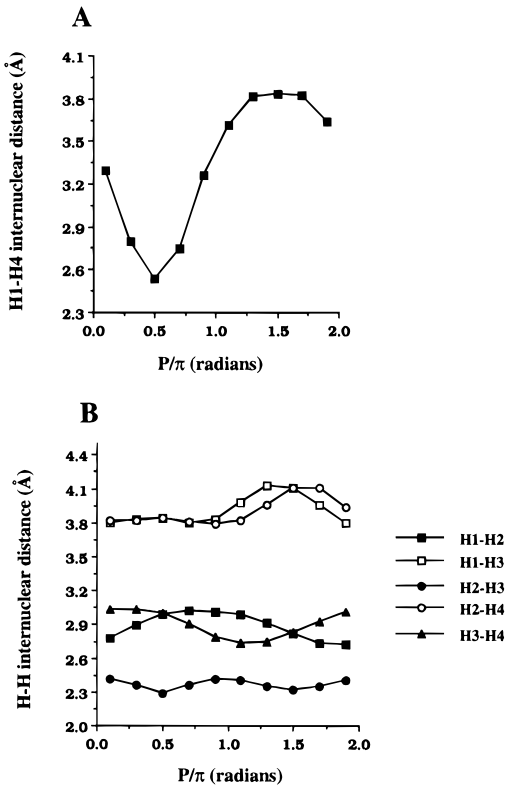

Figure 7. The effect of ring conformation of **2** on $^{1}H-^{1}H$ internuclear distances: (A) H1−H4; (B) H1−H2, H1−H3, H2−H3, H2−H4, and H3−H4.

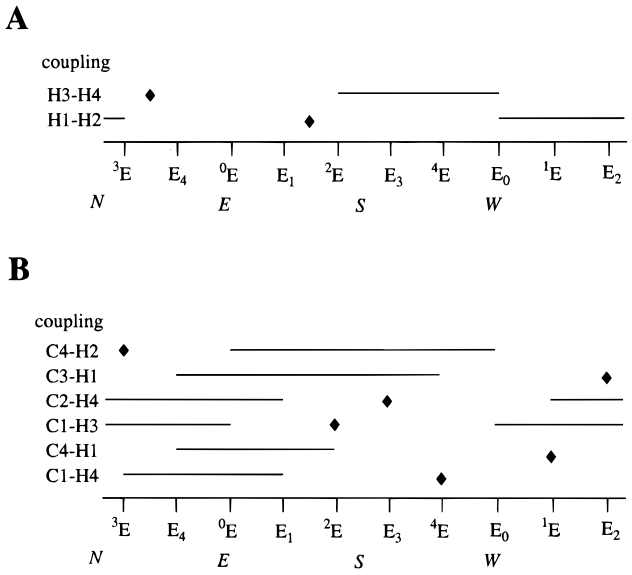

Figure 8. (A) A schematic representation of the response of $^{3}J_{HH}$ values in **2** to ring conformation. For each $^{3}J_{HH}$ value, maximal coupling is indicated by a ♦, whereas those conformers having miminal coupling are denoted by a solid line. (B) A similar representation of $^{3}J_{CH}$ behavior in **2** derived from data shown in Figure 10.

N/S ratios in solution.[10a,b] In contrast, $^{3}J_{H1,H2}$ and $^{3}J_{H3,H4}$ are small in northwest and southwest conformers, respectively. Pseudorotational regions exhibiting maximal and minimal $^{3}J_{HH}$ values in **2** are summarized in Figure 8A.

Seven intraring C−C−C−H and C−O−C−H torsions are found in **2**: C1−O4−C4−H4, C1−C2−C3−H3, C2−C3−C4−H4, C3−C2−C1−H1, C4−C3−C2−H2, C4−O4−C1−H1 and C5−C4−C3−H3. Their dependencies on ring conformation of **2**, obtained from MO-derived structures, are shown in Figure 9. The C5−C4−C3−H3 pathway shows torsional variations

(43) Jardetzky, O. *Biochem. Biophys. Acta* **1980**, *621*, 227−232.
(44) Homans, S. W. *Prog. NMR Spectrosc.* **1990**, *22*, 55−81.
(45) Haasnoot, C. A. G.; de Leeuw, F. A. A. M.; Altona, C. *Tetrahedron* **1980**, *36*, 2783−2792.

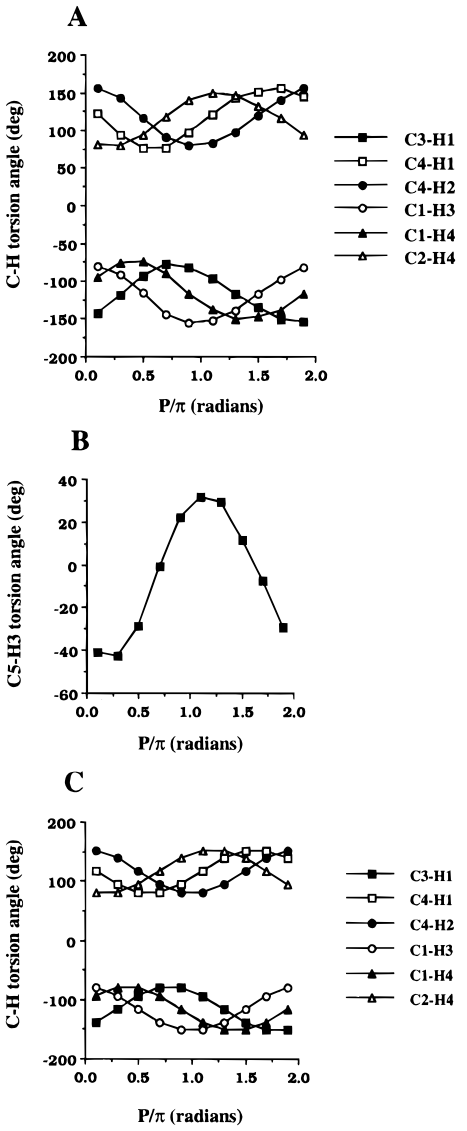

Figure 9. (A and B) C−H torsion angles in **2** as a function of ring conformation. (C) Computed torsion angles in **2** (see text).

Scheme 3. Assignment of Torsion Angles to the Endocyclic Bonds of **2**

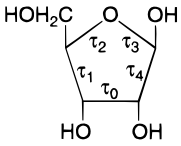

of ∼±40° (Figure 9B), and thus the change in $^3J_{C5,H3}$ is expected to be relatively small compared to that for the remaining $^3J_{CH}$; $^3J_{C5,H3}$ is likely to be a marginal conformational probe like $^3J_{H2,H3}$, both being cisoidal in nature. The remaining torsions vary from about 75° to 155° (absolute values) (Figure 9A). The behavior of the six C−H torsions involving *ring* carbons can be described by the relationship, torsion angle (in deg) = $\{-\cos[(P \times \pi) - 0.628\tau]37.3° + 116.5°\}(-1)^{\tau+1}$, where τ = 0, 1, 2, 3, and 4 for each endocyclic bond in the ring (Scheme 3), P = pseudorotation phase angle expressed in radians, and π = 180°. Thus, $\Theta_{C1,H3}$ (τ = 0) in the ^{3}E (P = 0.1) conformer = $\{-\cos[(0.1 \times 180°) - 0.628(0)]37.3° + 116.5°\}(-1)^{0+1}$ = −81.0°, which correlates well with the observed (MO) value of −80.5°. Observed (MO data) and calculated (using the above equation) C−H torsion angles (Figure 9C) are in close agreement.

Several Karplus curves for C−C−C−H and C−O−C−H coupling pathways in carbohydrates have been reported. In this study the curves developed by Schwarcz and Perlin[46] and Tvaroska *et al.*[47] were used, leading to the $^3J_{CH}$/conformation plots shown in Figure 10. These curves may be organized into four distinct groups: group 1 ($^3J_{C1,H3}$ and $^3J_{C2,H4}$); group 2 ($^3J_{C3,H1}$ and $^3J_{C4,H2}$); group 3 ($^3J_{C1,H4}$ and $^3J_{C4,H1}$); and group 4 ($^3J_{C5,H3}$). Curves in groups 1−3 show reasonable sensitivity to ring conformation, and thus the corresponding $^3J_{CH}$ values have potential as conformational probes. In contrast, the curve for $^3J_{C5,H3}$ has a limited amplitude and more complex dependency, thus making it less useful for structural applications. The data in Figure 10 are summarized in Figure 8B, where the six structurally-useful $^3J_{CH}$ values in **2** are compared with respect to maximal and minimal values along the pseudorotational itinerary (Scheme 1). A comparison of these data to those in Figure 8A shows that the dependencies of $^3J_{H1,H2}$ and $^3J_{C1,H3}$ on conformation are similar; likewise $^3J_{H3,H4}$ correlates with $^3J_{C4,H2}$. Thus, $^3J_{C1,H3}$ and $^3J_{C4,H2}$ might be used in a manner similar to that of their $^3J_{HH}$ counterparts in estimating N/S populations. More importantly, however, all of the $^3J_{CH}$ values show unique dependencies on conformation that, when considered collectively, may shed additional light on ring conformation in solution. For example, all of these couplings are at or near their minimal values in the ^{0}E conformation. Since it is difficult to establish the presence of a single ^{0}E form in solution using $^3J_{HH}$ values alone (due to the fact that the expected values of $^3J_{H1,H2}$ and $^3J_{H3,H4}$ are very similar for a pure ^{0}E model and for a model invoking ^{3}E/^{2}E exchange), the added information provided by $^3J_{CH}$ values can be helpful. It should be appreciated, however, that the maximal coupling values occur essentially within the western hemisphere of the pseudorotational itinerary for each $^3J_{CH}$, which is somewhat unfortunate since discrimination between some N/S models using $^3J_{CH}$ values may be compromised.

4. Validation of the Predicted Behavior of J_{CH} Values in 2 with Model Compounds. The change in C−H torsion angles in **2** as a function of ring conformation (Figure 9), determined via MO-derived structures, can be used to predict the behavior of $^3J_{CH}$ values in **2** (Figure 10) using appropriate Karplus relationships.[46,47] These latter correlations can, in principle, be applied to interpret experimentally-derived $^3J_{CH}$ values in **2** in structural terms, as discussed below. A similar approach cannot, however, be employed to assess the sensitivity of $^1J_{CH}$ and $^2J_{CH}$ values to ring conformation. In order to address the latter, and also provide some experimental verification of the $^3J_{CH}$ correlations in Figure 10, a set of conformationally-rigid compounds was sought that contain C−H coupling pathways structurally related to those found in specific conformers of **2**. Conformationally-rigid furanose rings might appear most suited to the task; however, in order to restrict these rings to one or a few conformations, they must be "locked" with bulky substituents or cyclic appendages. The presence of these groups changes the solubility properties of the derivatives and potentially introduces ring strain that is likely to affect J_{CH} values. Faced with these limitations, we chose methyl aldopyranosides (i.e., *pyranosyl rings*) as model compounds, with the belief that their limitations are no more serious than those associated with protected furanose models. In addition, the pyranosides are more readily prepared with ^{13}C-enrichment, making the measurement of J_{CH} values straightforward, and have recently been found useful in the interpretation of $^2J_{CH}$ values in 2′-deoxyribonucleosides.[14]

(46) Schwarcz, J. A.; Perlin, A. S. *Can. J. Chem.* **1972**, *50*, 3667−3676.
(47) Tvaroska, I.; Hricovini, M.; Petrakova, E. *Carbohydr. Res.* **1989**, *189*, 359−362.

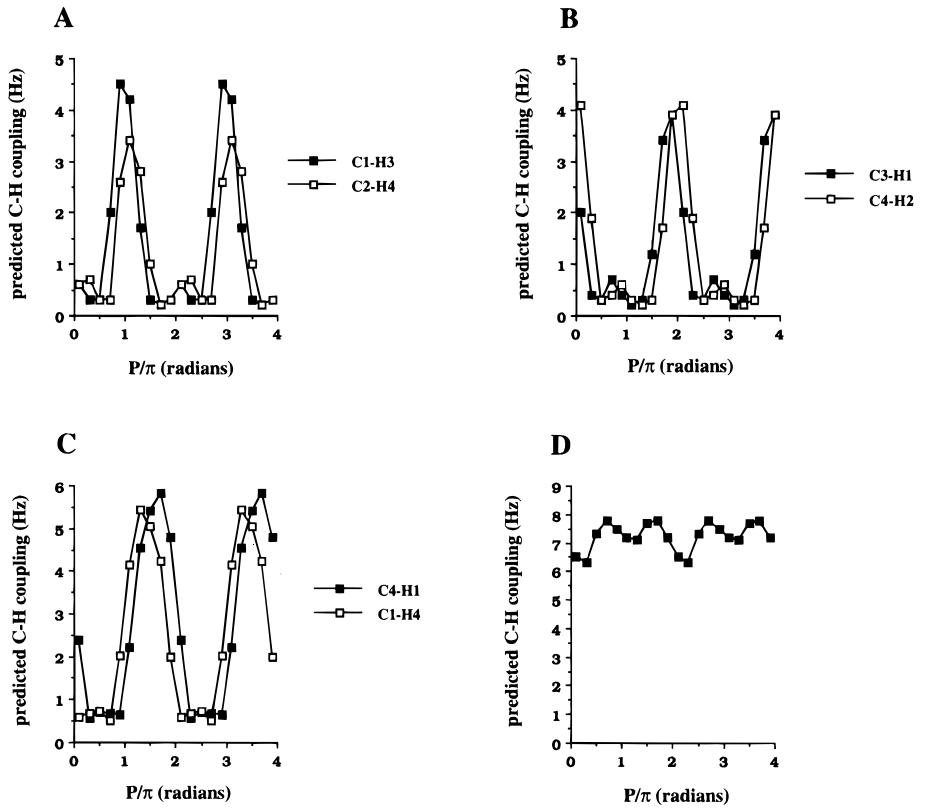

Figure 10. The effect of ring conformation of **2** on $^{3}J_{CH}$ values obtained from $^{3}J_{CCCH}$ and $^{3}J_{COCH}$ Karplus curves reported previously[46,47] and torsion angles obtained from MO-derived structures: (A) $^{3}J_{C1,H3}$ and $^{3}J_{C2,H4}$ (group 1); (B) $^{3}J_{C3,H1}$ and $^{3}J_{C4,H2}$ (group 2); (C) $^{3}J_{C4,H1}$ and $^{3}J_{C1,H4}$ (group 3); (D) $^{3}J_{C5,H3}$ (group 4).

Table 4. Predicted $^{13}C-^{1}H$ Spin-Couplings in North (E_2) and South (^2E) Forms of β-D-Ribofuranose **2**[a]

coupled nuclei	north (E_2) conformer	south (^2E) conformer
C1−H1	α-manno (171.0 Hz)	β-allo (163.4 Hz)
C1−H2	α-manno (∼−1.2 Hz)[c]	β-allo (−6.5 Hz)[c]
C1−H3	α-manno (0 Hz)	β-allo (6.0 Hz)
C1−H4 (NE,SW)[b]	β-gluco (2.3 Hz)[d]	β-arabino (7.6 Hz)[d]
C2−H1	α-manno (∼−1.8 Hz)[c]	β-allo (+0.3 Hz)[c]
C2−H2	α-manno (148.5 Hz)	β-allo (143.8 Hz)
C2−H3	α-manno (+1.4 Hz)[c]	β-allo (−4.8 Hz)[c]
C2−H4	β-allo (2.1 Hz)[e]	β-arabino [∼5 Hz][e,k]
C3−H1	α-manno (4.6 Hz)	β-allo (0 Hz)
C3−H2	α-manno (−3.7 Hz)	β-allo (+1.3 Hz)[c]
C3−H3	α-manno (146.5 Hz)	β-allo (149.8 Hz)
C3−H4	α-gluco (∼−3.1 Hz)[f]	α/β-arabino [∼−4 Hz][f]
C4−H1 (E,W)[b]	β-gluco (0 Hz)[g]	β-arabino (6.1 Hz)[g]
C4−H2	β-allo [∼5 Hz][h]	α-arabino [<1 Hz][h]
C4−H3	β-gluco (−4.8 Hz)[i]	α-arabino [∼5 Hz][i]
C5−H3 (NE,SW)[b]	β-gluco (3.5 Hz)[j]	1,6-anhydro-altro [∼3.5 Hz][j]

[a] Estimated from model methyl D-aldopyranosides. [b] Model compounds mimic the nonplanar forms in parentheses. [c] Coupling sign was determined by the crosspeak displacement method.[18,19] [d] Model coupling: $^{3}J_{C1,H5}$ (*gluco*) and $^{3}J_{C1,H5(equatorial)}$ (*arabino*). [e] Model coupling: $^{3}J_{C3,H5}$ (*gluco*) and $^{3}J_{C3,H5(equatorial)}$ (*arabino*). [f] Model coupling: $^{3}J_{C4,H5}$ (*gluco*) and $^{3}J_{C4,H5(equatorial)}$ (*arabino*). [g] Model coupling: $^{3}J_{C5,H1}$. [h] Model coupling: $^{3}J_{C5,H3}$. [i] Model coupling: $^{2}J_{C5,H4}$. [j] Model coupling: $^{3}J_{C6,H4}$. [k] Couplings in brackets are predicted by the projection rule.[49]

A series of model aldopyranosides was selected which provides crude estimates of $^{1}J_{CH}$, $^{2}J_{CH}$, and $^{3}J_{CH}$ values in N and S forms of **2** (Table 4).[17] For example, the relative disposition of hydroxyl substituents at C1, C2, and C3 in the E_2 (north) conformer of **2** is quasi-axial−quasi-axial−quasi-equatorial; a similar relative disposition is observed in methyl α-D-mannopyranoside **4** (axial−axial−equatorial) (Scheme 4). A comparison of structural parameters obtained via X-ray analysis of **3** (this paper) and **4** reveals similar (but not identical) values for bond lengths, angles, and torsions (Table 5). Thus, $^{2}J_{C1,H2}$ and $^{3}J_{C1,H3}$ in **4**, for example, provide reasonable *estimates* of the corresponding couplings in **2**. By the same argument, methyl β-D-allopyranoside **5** contains the same relative orientation of hydroxyl substituents at C1, C2, and C3 (equatorial−equatorial−axial) as found in the ^2E (south) conformer of **2**.

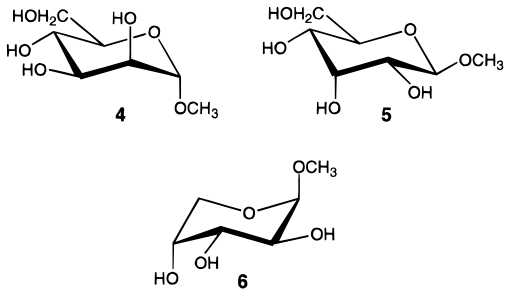

$^{13}C-^{1}H$ couplings in **2** involving C4 and C5 and their attached protons (and couplings involving C2 and C3 and protons attached to C4 and C5) cannot be estimated using the corresponding couplings in aldopyranosides, as C4 and C5 in **2** translate into C5 and C6 in aldohexopyranosides. Thus, for example, an estimate of $^{3}J_{C2,H4}$ in the S form of **2** was obtained from $^{3}J_{C3,H5(equatorial)}$ in methyl β-D-arabinopyranoside **6** ($^{1}C_4$ conformer) (Scheme 5, Table 4). In this and related cases (Table 4), the substitution patterns along the coupling pathways in the model compounds differ somewhat from those in **2**, resulting in somewhat greater error in these estimations.

Inspection of the model coupling data (Table 4) allows an assessment of the ability of specific $^{13}C-^{1}H$ couplings to distinguish between N and S forms of **2**. For example, $^{2}J_{C1,H2}$ differs significantly in N and S forms, whereas $^{2}J_{C2,H1}$ changes

Scheme 4

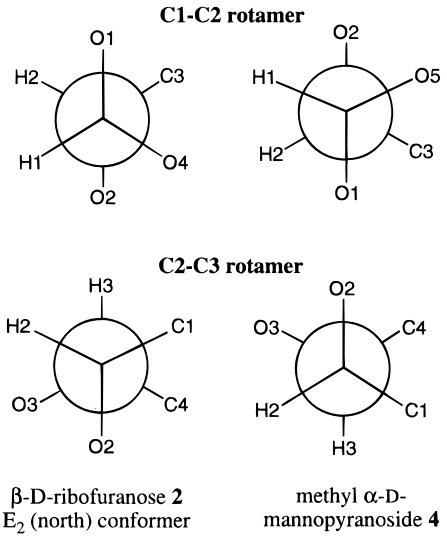

β-D-ribofuranose **2**
E_2 (north) conformer

methyl α-D-mannopyranoside **4**

Table 5. Crystal Structure Data for Methyl α-D-Mannopyranoside **4**[a] and Methyl *β*-D-Ribofuranoside **3**

parameter	α-*manno*	*β-ribo*
Bond Lengths (Å)		
C1−O1	1.400	1.419
C1−C2	1.524	1.515
C2−O2	1.415	1.412
C3−O3	1.421	1.412
C2−C3	1.529	1.526
Bond Angles (deg)		
O1−C1−C2	107.4	107.5
C2−C3−O3	109.9	115.5
O2−C2−C3	111.4	109.0
O3−C3−C4	108.7	113.8
C1−C2−C3	110.3	101.3
C2−C3−C4	110.6	103.2
Bond Torsions (deg)		
C1−C2−C3−H3	65.8	85.7
H1−C1−C2−C3	171.2	156.9
O1−C1−C2−O2	171.5	160.6
O2−C2−C3−O3	−55.5	−40.5
H1−C1−C2−H2	−69.0	−80.6
H2−C2−C3−H3	−53.7	−33.0

[a] Data taken from ref 52.

only slightly. Among the eleven couplings for which experimental data are available from model compounds (Table 4), ten experience a moderate to large change between N and S forms, making them potentially useful as conformational probes; only $^2J_{C2,H1}$ is predicted to be ineffective within this group. Interestingly, some of the two-bond $^{13}C-^1H$ couplings differ not only in *absolute* magnitude but also in *sign* in N and S forms;[48,49] for example, $^2J_{C2,H3}$ is positive in N forms (+1.4 Hz) and negative in S forms (−4.8 Hz), whereas the opposite is observed for $^2J_{C3,H2}$. Thus, sign determinations for these couplings will be important when attempting interpretation in conformational terms; Tinoco and co-workers have recently drawn similar conclusions.[20,21] Our *predicted* (via empirical rules[49]) signs for the $^2J_{CH}$ values in the *β-ribo* ring (Table 4) agree with those reported previously[20,21] except for $^2J_{C2,H1}$, which we predict to be zero in both N and S forms rather than negative.

It is useful to compare the $^3J_{CH}$ model coupling data in Table 4 (i.e., $^3J_{C1,H3}$, $^3J_{C2,H4}$, $^3J_{C3,H1}$, and $^3J_{C5,H3}$) to that derived via MO-derived torsion angles and "standard" Karplus relationships

(48) Schwarcz, J. A.; Cyr, N.; Perlin, A. S. *Can. J. Chem.* **1975**, *53*, 1872−1875.
(49) Bock, K.; Pedersen, C. *Acta Chem. Scand.* **1977**, *B31*, 354−358.

Scheme 5

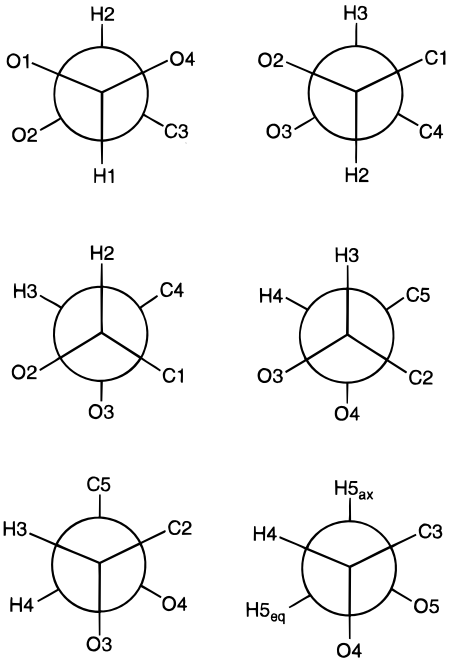

β-D-ribofuranose **2**
^2E (south) conformer

methyl β-D-arabinopyranoside **6**

for appropriate conformers (Figure 10). In all cases, the trends observed in the model $^3J_{CH}$ data are consistent with those observed for computed $^3J_{CH}$ data, although differences in absolute magnitude are observed. In general, the model couplings are larger than the computed couplings, as expected, since torsion angles in the model compounds of ∼60° and ∼180° are smaller and larger, respectively, than the corresponding torsions encountered in **2** (Table 5). Thus, the differences in $^3J_{CH}$ values for N and S forms predicted from the model compounds probably represent upper limits.

5. Computed Behavior of $^1J_{CH}$, $^2J_{CH}$, and $^3J_{CH}$ in 2. The data shown in Table 4 provide an assessment of the magnitude of change in $^1J_{CH}$ and $^2J_{CH}$ values in **2** expected between N and S forms, but they do not provide information about these couplings in other conformers. The latter information was obtained by computing these couplings from HF/6-31G* structures using methods described earlier.[40b,41,50]

$^1J_{CH}$ values in aldofuranosyl rings have been shown recently to depend on C−H bond lengths, with shorter bonds yielding larger couplings.[41] C−H bond lengths vary systematically with bond orientation; that is, a given C−H bond length is minimal when quasi-equatorial and maximal when quasi-axial. This trend is observed in **2** (Figure 11A). For example, $^1J_{C1,H1}$ and $^1J_{C4,H4}$ are minimal in east forms and maximal in southwest forms, as expected based on bond length considerations (Figure 2A). In contrast, $^1J_{C2,H2}$ is minimal in S forms and maximal in N forms, again consistent with bond length behavior (Figure 2B). As discussed previously,[41] the behavior of the C3−H3 bond length is unusual and is apparently caused by C3−O3 bond rotation through the pseudorotational itinerary which orients a lone-pair orbital on O3 antiperiplanar to the C3−H3 bond in S forms but not in N forms; this rotation is apparently driven by the formation of an intramolecular H-bond between O2 and O3 in S forms. This antiperiplanar arrangement acts to *elongate* the C3−H3 bond and thus counteracts the intrinsic *shortening* that would otherwise occur in S forms (since the C3−H3 bond

(50) Carmichael, I.; Chipman, D. M.; Podlasek, C. A.; Serianni, A. S. *J. Am. Chem. Soc.* **1993**, *115*, 10863−10870.

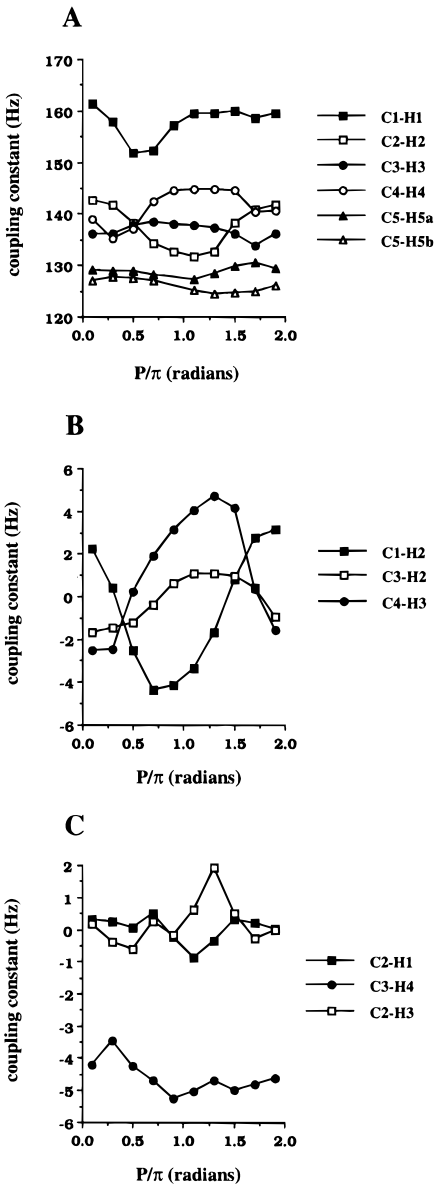

Figure 11. (A) Computed $^{1}J_{CH}$ values in **2** as a function of ring conformation. (B) Computed $^{2}J_{CH}$ values in **2** which are sensitive to ring conformation. (C) Computed $^{2}J_{CH}$ values in **2** which are insensitive to ring conformation.

is quasi-equatorial in these conformers). For this reason, the C3−H3 bond length is maximal in S forms (where it is quasi-equatorial) and minimal in N forms (where it is quasi-axial) (Figure 2B). Interestingly, computed $^{1}J_{C3,H3}$ values in **2** (Figure 11A) *increase* slightly in S forms; if bond length were the sole determinant of $^{1}J_{CH}$, a *decrease* in $^{1}J_{CH}$ in S forms similar to that observed for C2−H2 might be expected. This result suggests that C−H bond *orientation* may play a greater role in determining $^{1}J_{CH}$ than C−H *bond length*; thus, although the C3−H3 bond lengthens in S forms, its quasi-equatorial orientation in S forms dictates an increase in $^{1}J_{CH}$, albeit a smaller increase than expected in the absence of lone-pair effects. We also cannot, at present, assess the indirect effects on $^{1}J_{C3,H3}$ caused by hydrogen bonding in S forms.

Similar calculations were conducted to evaluate changes in $^{2}J_{CH}$ values in **2** as a function of ring conformation (Figure 11B,C). Large *absolute* changes in coupling are observed for $^{2}J_{C1,H2}$ and $^{2}J_{C4,H3}$, whereas changes in $^{2}J_{C3,H2}$ are more modest. More importantly, the trends predicted from these computations are consistent with those based on the aldopyranoside model couplings (Table 4). Thus, for example, $^{2}J_{C1,H2}$ values become increasingly negative as N forms convert to S forms; the model compounds indicate a change from −1.2 to −6.5 Hz. $^{2}J_{C2,H1}$ and $^{2}J_{C3,H4}$ are relatively insensitive to ring conformation, which is also consistent with the model studies (Table 4). The behavior of $^{2}J_{C2,H3}$ is, however, anomalous, since model studies suggest this coupling should become increasingly negative as N forms convert to S forms, yet the computed behavior shows no clear trend in this direction (Figure 11C). This behavior might be attributed to the effects of C3−O3 bond rotation (and intramolecular H-bonding) on the C3−H3 bond (see above) which may influence not only $^{1}J_{C3,H3}$ (see above) but also $^{2}J_{C2,H3}$.

Although the use of C−H torsion angles derived from MO calculations (Figure 9) and appropriate Karplus relationships[46,47] may be used to evaluate the sensitivity of particular $^{3}J_{CH}$ values in **2** to ring conformation (Figure 10), similar data were also obtained via calculation (Figure 12). Both data sets reveal the same general trends, although curve amplitude varies between the two treatments. This variability originates from the limitations of the Karplus curves employed and/or the computational methods used to calculate the couplings.

6. Comparison with Experiment. To date, few studies have been reported in which J_{CH} values in β-D-ribofuranosyl rings have been measured and/or interpreted. Some data are available for glycofuranosides,[12,16] nucleosides,[12,13] and an RNA UUGA hairpin.[21] We examine these available data in light of the coupling predictions made above for **2**, with the realization that **2** is not a perfect mimic of the β-D-ribofuranosyl ring of ribonucleosides(tides), being an *O*-glycoside rather than an *N*-glycoside.

We focus first on several simple model compounds, adenosine[12] **7**, erythroadenosine[13] **8**, methyl β-D-ribofuranoside[12] **3**, and methyl β-D-erythrofuranoside[13,16] **9** (Table 6). $^{3}J_{H1',H2'}$ and $^{3}J_{H3',H4'}$ observed in **7** and **9** suggest the presence of comparable proportions of N and S forms; in contrast, data for **3** support a preference for N forms, while that for **8** indicate a preference for S forms. Note that $^{3}J_{H2',H3'}$ is relatively constant in these compounds, providing evidence of its relative insensitivity to different proportions of N and S forms in solution.

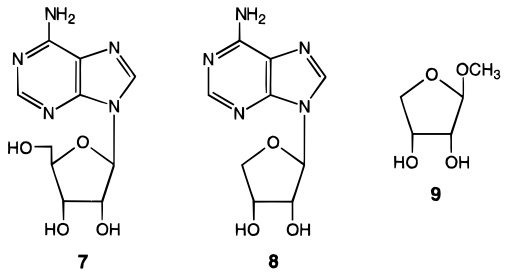

Several J_{CH} values measured in **3**, **7**, **8**, and **9** were assessed with respect to their consistency with the above conformational models. $^{2}J_{C1',H2'}$ for **7** and **9** are similar and have the magnitude and sign expected for a N/S equilibration. A more *negative* $^{2}J_{C1',H2'}$ is observed in **8** than in **7** and **9**, as expected if S forms are more preferred in the former. The zero value of $^{2}J_{C1',H2'}$ in **3** is consistent with a preference for N forms. Good internal consistency is also observed for $^{3}J_{C1',H3'}$; for example, $^{3}J_{C1',H3'}$ = 5.2 Hz in **8** which prefers S forms, whereas this coupling is 0.9 Hz in **3** where N forms predominate and takes an intermediate value in **7** and **9** where N and S forms are present in comparable proportions. The available data for $^{3}J_{C3',H1'}$ also show the expected behavior, being larger for **3** (N preference) than for **9** (N/S mix).

The remaining three J_{CH} values considered in Table 6 ($^{2}J_{C2',H1'}$, $^{2}J_{C2',H3'}$, and $^{3}J_{C2',H4'}$) require more extended discussion. $^{3}J_{C2',H4'}$ values in **3** and **7** are similar despite different confor-

Table 6. $^{1}H-^{1}H$ and $^{13}C-^{1}H$ Spin-Coupling Data in Furanosides, Erythronucleosides, and Ribonucleosides

coupled nuclei	adenosine **7**[a]	erythroadenosine **8**[b]	methyl β-D-ribofuranoside **3**[b]	methyl β-D-erythrofuranoside **9**[c]
H1−H2	6.2	6.7	1.2	2.9
H2−H3[d]	5.3	4.6	4.6	4.8
H3−H4[e]	3.3	1.7	6.9	3.5
model	N/S	S	N	N/S

coupled nuclei	ribonucleosides[a]	erythroadenosine **8**[b]	methyl β-D-ribofuranoside **3**[b]	methyl β-D-erythrofuranoside **9**[c]	coupling range[f]
C1, H2	-2.5 ± 0.7	−4.1	0	−2.4	−1.2, −6.5
C1, H3	4.1 ± 1.0	5.2	0.9	3.9	0, 6.0
C2, H1	-3.3 ± 0.2		br[g]	br	−1.8, 0.3
C2, H3	0		1.4	0	1.4, −4.8
C2, H4	1.4 ± 0.2		0.7	3.5[e]	
C3, H1			3.1	1.9	4.6, 0

[a] Average couplings in adenosine, cytidine, guanosine, and uridine; data from ref 12. [b] Data from ref 12. [c] Data from ref 16. [d] Coupling is insensitive to N/S conformational interconversion (see text). [e] Coupling pertains to the H4*S* proton in erythroadenosine and methyl β-D-erythrofuranoside. [f] Predicted from model hexopyranosides: first value, N forms; second value, S forms. [g] Denotes broadened signal ($J < 0.8$ Hz).

mational preferences. The small value for **3** (0.7 Hz) is consistent with expectations, whereas that for the ribonucleosides appears small. However, N/S averaging in the latter can produce a small value for $^{3}J_{C2',H4'}$ if ^{3}E and ^{2}E are the forms in chemical exchange (Figure 10A). Only a small difference in coupling magnitude distinguishes a N-preference model from a N/S mix model. Thus, small $^{3}J_{C2',H4'}$ values observed in the UUGA hairpin (1.0−1.6 Hz)[21] do not, by themselves, indicate a highly-preferred ^{3}E (C3′-*endo*) sugar conformation, contrary to arguments made previously.[21] Interestingly, $^{3}J_{C2,H4} = 3.5$ Hz in **9**, which is significantly different from $^{3}J_{C2',H4'}$ in ribonucleosides despite the same N/S conformational behavior. This result illustrates the importance of substituent effects on $^{3}J_{CH}$ values. Substitution of an H for CH_2OH at C4 apparently changes the Karplus curve enough to render direct comparison between **7** and **9** invalid. The available data indicate that such a substitution *increases* the observed coupling for a given C2−C3−C4−H4 dihedral angle.

The observed value of $^{2}J_{C2',H3'}$ in **3** (1.4 Hz; presumably positive) is not significantly different from the observed values in **7** and **9** (0 Hz). The latter, however, may actually be nonzero (<1.0 Hz) and have a negative sign, making the difference more consistent with expectations. Since $^{2}J_{C2',H3'}$ could not be measured in **8**, we cannot evaluate its magnitude and sign in S forms and thus assess the sensitivity of this coupling to different N/S models. In the UUGA RNA hairpin,[21] however, residues preferring S forms reveal $^{2}J_{C2',H3'}$ of −1.9 to −2.4 Hz.

$^{2}J_{C2',H1'}$ values in **3** (br) and **9** (br) are not unexpected, since the predicted difference in this coupling in N and N/S models is small (Table 4, Figure 11C). However, $^{2}J_{C2',H1'}$ values in ribonucleosides (-3.3 ± 0.2 Hz, sign established experimentally[18,19]) deviate significantly from the predicted range for these couplings (Table 4); similar couplings in magnitude and sign are observed in the UUGA hairpin.[21] This behavior suggests that the substitution of the nitrogen base at C1′ alters the C2−C1−H1 coupling pathway sufficiently from the *O*-glycoside models to render the estimated limits invalid. Given the fact the $^{2}J_{C1',H2'}$ behaves reasonably well (see above), these results suggest that a change in electronegative substitution at the carbon bearing the coupled proton has a greater effect on $^{2}J_{CH}$ values than the same change made at the coupled carbon, at least for carbons bearing two electronegative substituents (e.g., C1′), but this argument will require further experimental validation.

Conclusions

The primary objective of this investigation was to assess the dependencies of J_{CH} values in the β-D-ribofuranose ring **2** on ring conformation, with the expectation that a more quantitative understanding of these relationships will lead to an improved means of assessing the solution conformation of these rings, either as free entities or as constituents of more complex biomolecules. The present study represents an extension of earlier work[12] in which J_{CH} values involving C1′ and C2′ were measured in several ^{13}C-labeled ribonucleosides and interpreted in a qualitative fashion in terms of preferred furanose conformation. Inspection shows that 17 one-, two-, and three-bond $^{13}C-^{1}H$ spin-couplings in **2** could, in principle, be affected by ring conformation (Table 1). The results of the present study identify those couplings which respond sufficiently to changes in ring shape to warrant further development as conformational probes. Key results and conclusions may be summarized as follows:

(a) *Ab initio* MO data on **2** yields a conformational energy profile in which an N form (E_2) is favored. The puckering amplitude (τ_m) is not constant throughout the pseudorotational itinerary but reaches maximal and minimal values in the eastern and western regions, respectively. This latter behavior is consistent with predictions made earlier by Levitt and Warshel[1b] and with results from molecular dynamics simulations by Harvey and Prabhakaran.[5a]

(b) Crystal structure data obtained on the methyl glycoside of **2** (i.e., **3**) yield structural parameters similar, but not identical, to those derived from *ab initio* MO calculations. In general, computations conducted at the MP2/6-31G* level of theory give bond lengths, bond angles, and bond torsions in closer agreement with crystal data than HF/6-31G* data. The largest bond length deviations between X-ray and MO data occur for C−O bonds.

(c) C−H torsion angles in **2** vary systematically with ring conformation. Using these torsion angles and previously derived Karplus relationships,[46,47] six of the seven available $^{3}J_{CH}$ values within the ring of **2** were found to change substantially with ring conformation ($^{3}J_{C1,H3}$, $^{3}J_{C1,H4}$, $^{3}J_{C2,H4}$, $^{3}J_{C3,H1}$, $^{3}J_{C4,H1}$, and $^{3}J_{C4,H2}$); $^{3}J_{C5,H3}$, being cisoidal in nature like $^{3}J_{H2,H3}$, appears less reliable as a conformational probe. The six conformationally-sensitive $^{3}J_{CH}$ values can be grouped into three categories based on their response to conformation (group 1, $^{3}J_{C1,H3}$ and $^{3}J_{C2,H4}$; group 2, $^{3}J_{C3,H1}$ and $^{3}J_{C4,H2}$; group 3, $^{3}J_{C1,H4}$ and $^{3}J_{C4,H1}$) (Figures 10 and 12). In general, coupling complementarity is observed between groups 1 and 2; that is, group 1 couplings are small in N forms and large in S forms, whereas the opposite is observed in group 2. This behavior is related to the complementarity observed between $^{3}J_{H1,H2}$ and $^{3}J_{H3,H4}$ in **2**, which provides the basis for their use in estimating N/S proportions. A similar quantitative application of appropriate $^{3}J_{CH}$ pairs is thus anticipated.

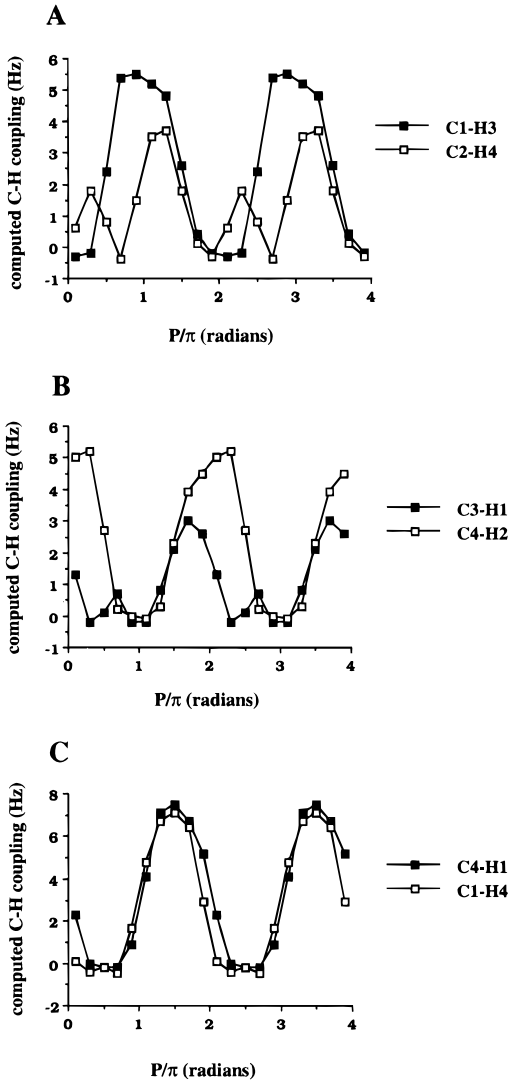

Figure 12. Computed $^{3}J_{CH}$ values in **2** as a function of ring conformation: (A) $^{3}J_{C1,H3}$ and $^{3}J_{C2,H4}$ (group 1); (B) $^{3}J_{C3,H1}$ and $^{3}J_{C4,H2}$ (group 2); (C) $^{3}J_{C4,H1}$ and $^{3}J_{C1,H4}$ (group 3).

(d) Several $^{2}J_{CH}$ values within the ring of **2** change significantly in magnitude and/or sign with conformation (Figure 11B,C). Of the six available two-bond $^{13}C-^{1}H$ spin-couplings in **2**, three appear valuable as structural probes: $^{2}J_{C1,H2}$, $^{2}J_{C3,H2}$, and $^{2}J_{C4,H3}$. Two of the remaining three ($^{2}J_{C2,H1}$ and $^{2}J_{C3,H4}$) appear to be relatively insensitive to ring shape, while data for $^{2}J_{C2,H3}$ are inconclusive.

(e) $^{1}J_{CH}$ values in **2** vary with conformation according to the orientation of the respective C−H bond (Figure 11A). Data for $^{1}J_{C1,H1}$, $^{1}J_{C2,H2}$, and $^{1}J_{C4,H4}$ indicate that coupling is maximal for quasi-equatorial C−H bonds and minimal for quasi-axial C−H bonds. It should be appreciated, however, that $^{13}C-^{1}H$ coupling behavior involving H1 in nucleosides(tides) may differ from that observed in this study, since the model compounds used herein (Table 4) were *O*-glycosides rather than *N*-glycosides; $^{13}C-^{1}H$ couplings involving other ring protons may also be affected by different substitution at C1 but to a lesser extent.

The combined use of computed J_{CH} values and conformationally-rigid model compounds (methyl aldopyranosides) provides a reasonable means to arrive at a semi-quantitative treatment of $^{13}C-^{1}H$ coupling behavior within aldofuranosyl rings. In most cases, general trends in coupling behavior predicted from calculated couplings were consistent with experimental observations made with the models. However, while the general trends are internally consistent and thus reassuring, the agreement in terms of absolute magnitudes of couplings is modest in most cases. Thus, while the present study provides reliable results in terms of *coupling trends*, the available data are not yet sufficient for use in quantitative determinations of conformational behavior in solution. It should be appreciated, however, that all of the furanosyl rings within RNA have the same configuration, and thus a knowledge of coupling trends alone can be valuable when comparing corresponding J_{CH} values in different residues.

In this study, we examined one conformation representing each envelope form of **2**. In solution, however, conformational interconversions will likely occur not only between fundamental ring forms (pseudorotation), but also within a given form (i.e., changes in puckering amplitude, rotations about exocyclic C−O and C−C bonds). These motions will modulate the observed couplings within a given form of the ring and will ultimately need to be taken into account in the quantitative interpretation of J_{CH} values.

Chemi-enzymic methods are presently available to prepare nearly all of the ^{13}C isotopomers of **2**,[26] thus providing access to a wide range of ^{13}C-labeled ribonucleosides[12] for use in constructing specific-sequence RNAs.[22] A variety of NMR methods is currently available to measure J_{CH} values in ^{13}C-labeled RNAs.[51] The fundamental $^{13}C-^{1}H$ spin-coupling behavior discussed in this paper may prove useful in the interpretation of J_{CH} values within the β-D-ribofuranosyl rings of RNA in conformational terms.

Acknowledgment. The research reported herein has been supported by the Office of Basic Energy Sciences of the United States Department of Energy, and Omicron Biochemicals, Inc. of South Bend, IN. This is Document No. NDRL-3842 from the Notre Dame Radiation Laboratory.

Supporting Information Available: A table of positional and equivalent isotropic thermal parameters for methyl β-D-ribofuranoside **3** (3 pages). This material is contained in many libraries on microfiche, immediately follows this article in the microfilm version of the journal, can be ordered from the ACS, and can be downloaded from the Internet; see any current masthead page for ordering information and Internet access instructions.

JA9519647

(51) Biamonti, C.; Rios, C. B.; Lyons, B. A.; Montelione, G. T. *Adv. Biophys. Chem.* **1994**, *4*, 51−120.
(52) Jeffrey, G. A.; McMullan, R. K.; Takagi, S. *Acta Crystallogr.* **1977**, *B33*, 728−737.